

INTRA-BEAM SCATTERING MEASUREMENTS IN RHIC*

W. Fischer[†], R. Connolly, S. Tepikian, J. van Zeijts, K. Zeno, BNL, Upton, NY 11973, USA

Abstract

RHIC in gold operation shows significant intra-beam scattering due to the high charge state of the stored ions. Intra-beam scattering leads to longitudinal and transverse emittance growth. The longitudinal emittance growth causes debunching in operation; the transverse emittance growth contributes to the reduction of the beam and luminosity lifetimes. The longitudinal and transverse beam growth was measured. Beam growth measurement are compared with computations.

1 INTRODUCTION

Intra-beam scattering [1, 2] can cause emittance growth in all beam dimensions and limit the performance of hadron [3] and lepton machines [4]. To compute the beam size evolution from intra-beam scattering, a number of computer codes were developed and tested with beam measurements [4-9]. With heavy ion beams at energies not attained thus far, the Relativistic Heavy Ion Collider (RHIC) [10] allows the measurement of intra-beam scattering in a new parameter range (see Tab. 1).

All measurements reported here observe the free expansion of the beam in the longitudinal and transverse dimensions. These observations are compared with simulation as described in Ref. [3]. Only FODO cells are included in the simulation. We compare the bunch length and transverse emittances as a function of time instead of growth rates. This avoids the possibly large error in determining a derivative of a experimental signal that is not smooth. Beam measurements were done at injection energy, below transition, and at storage energy, above transition.

2 BEAM SIZE MEASUREMENTS

Longitudinal The bunch length and bunched beam current is measured with a wall current monitor with 0.25 ns resolution (see Fig. 1). At injection a measurement of all bunches is taken every 12 s, during stores every 5 min. The

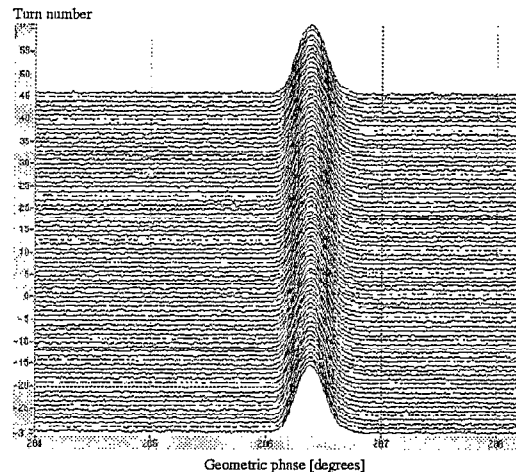


Figure 1: Bunch length measurement with a wall current monitor. A geometric phase difference of one degree corresponds to one bucket length at injection.

beam profiles are fitted to a Gaussian distribution and the fitted bunch lengths are averaged over all bunches.

Transversal Different methods are used at injection and storage energy to measure the transverse beam size. At injection, the beam size is obtained from an ionization profile monitor (IPM). The observed profiles (see Fig. 2) are fitted to a Gaussian distribution. Profiles are typically taken every half minute. However only the vertical IPM returned reliable profiles and we assume equal transverse emittances in both planes. The transverse planes are coupled with a typical minimum tune approach of $\Delta Q_{min} = 0.01$.

At storage energy the transverse beam size is derived from the luminosity signals and the bunched beam currents (see Fig. 3). This allows to analyze all available store data for emittance growth. IPM data are not available in all cases. We assume equal emittances in both planes and both rings. The time dependent emittance $\epsilon(t)$ is derived as

$$\epsilon(t) = f \frac{N_B(t) N_Y(t)}{L(t)} \quad (1)$$

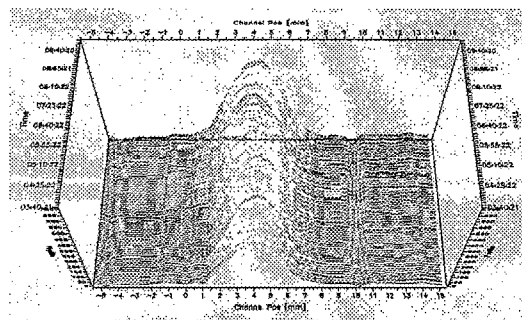


Figure 2: Time evolution of the transverse beam size as recorded by the ionization profile monitor.

* Work supported by US DOE under contract DE-AC02-98CH10886.

[†] Wolfram.Fischer@bnl.gov

Table 1: Parameters for Au⁷⁹⁺ and p⁺ beams in Run 2001.

parameter	unit	Au ⁷⁹⁺	Au ⁷⁹⁺	p ⁺
		injection	store	store
relativistic gamma	...	10.5	107	107
no. of bunches	...	55	55	55
ions per bunch N_b	...	0.25...0.7 · 10 ⁹		10 ¹¹
rms emitt. $\epsilon_{N x,y}$	μm	2.0	2.5	3.5
harmonic no. h	...	360	7×360	360
gap voltage V	MV	0.3	3.0	0.3
rms bunch area S	eV·s/u	0.08	0.08	0.16

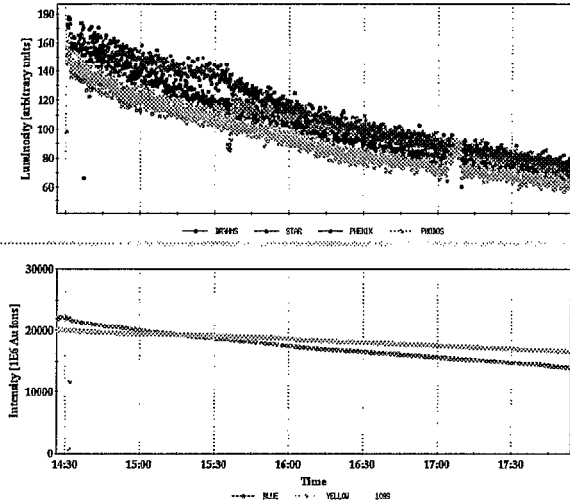


Figure 3: Luminosity signals from all four experiments (upper part) and bunched beam currents of Blue and Yellow beam (lower part) as a function of time during a store.

where L is the event rate, and N_B, N_Y are the Blue and Yellow bunched intensities respectively. The factor f is determined experimentally using ionization profile monitor data and the measured beam-beam tune shift [11], when available. Event rates from all four experiments are used.

3 MEASUREMENTS AT STORE

Above transition intra-beam scattering causes continuous beam growth in all dimension, no equilibrium exists. Measurements reported here were taken with $\beta^* = 5$ m in all interaction points. Measurements at smaller β^* were excluded since a significantly larger transverse growth was observed for comparable intensities, likely to stem from interaction region triplet errors. Gold measurements can be compared with protons (Tabs. 1 and 2), for which growth rates are reduced by an order of magnitude.

22 stores of gold beams with a total of 2420 bunches were analyzed over a period of 90 min. The time was chosen to observe a strong effect and to maximize the amount of available data. A typical store in operation lasts about 5

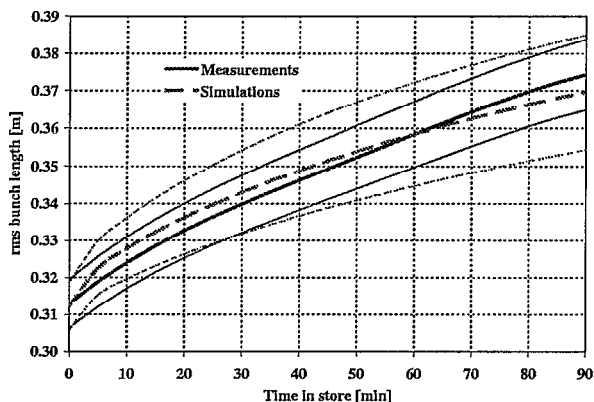


Figure 4: Bunch length growth in gold stores. The thick lines in the middle show the average over 22 stores, the thin lines the deviation of one standard error.

Table 2: Comparison of measured and computed average bunch length and emittance growth at store, in percent.

time in store [min]	30	60	90
bunch length growth			
Au, measured	8.6	14.3	19.6
Au, simulated	9.8	14.8	18.3
transverse emittance growth			
Au, measured	9.6	17.5	24.2
Au, simulated	7.4	12.7	16.8
p, measured	1.8	3.9	5.5

hours. The intensity ranged from $0.25 \cdot 10^9$ to $0.40 \cdot 10^9$ ions per bunch. Each of the 22 stores was simulated separately, starting with the initial intensities, transverse emittances, and average bunch length, and taking into account the observed beam losses over the observation period.

Figs. 4 and 5 compare the measured and computed bunch length and transverse emittance growth. The bunch length in the simulation grows faster initially, then slower than in the measurement. After 90 min there is good agreement (Tab. 2). The experimental distribution widens less than the one obtained in the simulation. Bunch length data from protons are only available with the accelerating rf system that has a lower harmonic number and gap voltage than the storage system, used for gold (Tab. 1). For protons only 2% bunch length growth was observed on average after 90 min.

The transverse emittance grows always faster in the measurement than in the simulation. At least part of the discrepancy can be attributed to effects that are not caused by intra-beam scattering. Such effects can be observed experimentally with proton beams (Tab. 2). However, the proton beams were larger and the beam-beam parameter was about twice as large as with gold beams. The proton emittance growth in Tab. 2 is derived from fitted luminosity and bunched beam lifetimes and is less precise than the reported emittance growth for gold beams.

4 MEASUREMENTS AT INJECTION

Below transition an equilibrium for the transverse and longitudinal emittances can exist, and the transverse emit-

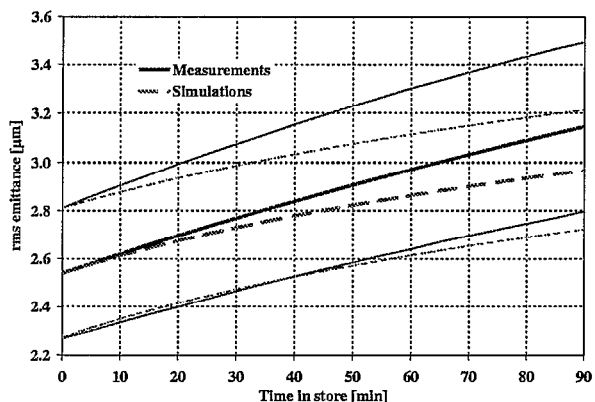


Figure 5: Transverse emittance growth in gold stores. The thick lines in the middle show the average over 22 stores, the thin lines the deviation of one standard error.

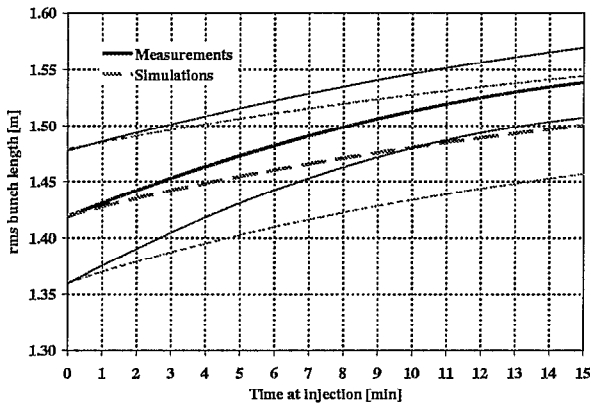


Figure 6: Bunch length growth at injection. The thick lines in the middle show the average over 8 stores, the thin lines the deviation of one standard error.

tances could shrink to increase the bunch length. At injection only the accelerating rf system is used and buckets are longer than at store (Tab. 1). The injection lattice has $\beta^* = 10$ m. There are no reliable proton data available at injection. Rest gas ionization is greatly reduced with protons, and the quality of IPM profiles suffers. Longitudinally, the beam showed sustained coherent oscillations at injection, which made measurements of bunch length growth difficult.

Only a limited number of measurements are available at injection: 8 bunch length and 7 transverse emittance growth measurements. Observations were extended over 15 min, about 3 times the time needed to inject beams in operation. The intensity ranged from $0.40 \cdot 10^9$ to $0.72 \cdot 10^9$ ions per bunch. The 8 cases in which bunch length growth was observed were simulated. In only 3 cases there are longitudinal and transverse data available at the same time. In these cases, the simulations were performed with the measured initial values. If no transverse data were available, the average initial value was substituted.

Figs. 6 and 7 compare the measured and computed bunch length and transverse emittance growth. The bunch length in the simulation grows slower than in the measurement. After 15 min there is good agreement (Tab. 3). The transverse emittance always grows substantially in the measurements while we expect a slight decrease from the simulations. The transverse emittance growth fits well to a function linear in time, typical of a random walk process for the betatron amplitudes. This suggests that a significant source of noise dominates the transverse emittance growth.

Table 3: Comparison of measured and computed average bunch length and emittance growth at injection, in percent.

time in store [min]	5	10	15
bunch length growth			
Au, measured	3.8	6.7	8.5
Au, simulated	2.5	4.3	5.7
transverse emittance growth			
Au, measured	10.2	20.5	30.7
Au, simulated	-1.6	-2.8	-3.8

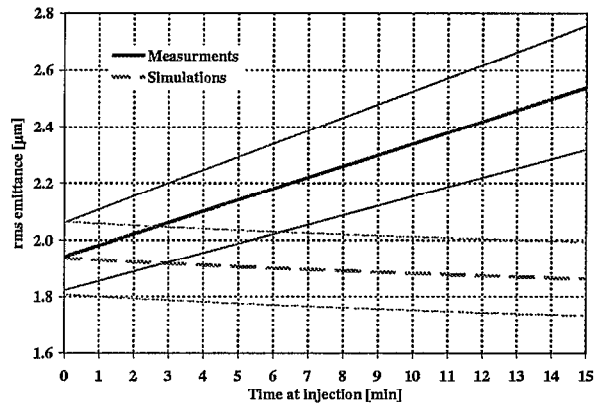


Figure 7: Transverse emittance growth at injection. The thick lines in the middle show the average over 7 stores, the thin lines the deviation of one standard error.

5 SUMMARY

The transverse and longitudinal emittance growth was measured with gold beams at store, above transition, and at injection, below transition. In both cases, measurements and simulations agree better for the bunch length than for the transverse emittance. At store, part of the discrepancy can be attributed to emittance growth effects that are not caused by intra-beam scattering. These were estimated with proton beam measurements. At injection, the transverse emittance growth may be dominated by a relatively strong source of noise.

6 ACKNOWLEDGMENTS

The authors would like to thank for support and discussion: J.M. Brennan, M. Blaskiewicz, P. Cameron, R. Lee, G. Parzen, F. Pilat, and J. Wei.

7 REFERENCES

- [1] A. Piwinski, "Touschek Effect and Intrabeam Scattering" in "Handbook of Accelerator Physics and Engineering" edited by A.W. Chao and M. Tigner, World Scientific (1999).
- [2] J.D. Bjorken and S.K. Mtingwa, "Intrabeam Scattering", Part. Accel. Vol. 13, pp. 115-143 (1983).
- [3] J. Wei, "Evolution of Hadron Beams under Intrabeam Scattering", PAC 93, Washington, D.C. pp. 3561 (1993).
- [4] K.L.F. Bane, H. Hayano, K. Kubo, T. Naito, T. Oguki, J. Urakawa, "Intrabeam Scattering Analysis of ATF Beam Measurements", PAC'01, Chicago, SLAC-PUB-8875 (2001).
- [5] M. Martini, "Intrabeam Scattering in the ACOI-AA Machines", CERN PS/84-9 (AA) (1984).
- [6] G. Parzen, "Intrabeam Scattering at High Energies", Nuc. Inst. Meth. A245, pp. 231-240 (1986).
- [7] M. Conte and M. Martini, "Intrabeam Scattering in the CERN Antiproton Accumulator", Part. Accel. 17, pp. 1-10 (1985).
- [8] L.R. Evans and J. Gareyte, PAC'85 (1985).
- [9] C. Bhat, L.K. Spentouris, P.L. Colestock, "Measurements of Intrabeam Scattering Rates below Transition in the Fermilab Antiproton Accumulator", PAC'99, New York (1999).
- [10] F. Pilat, "RHIC Status and Plans", these proceedings.
- [11] W. Fischer, P. Cameron, S. Peggs and T. Satogata, "Tune modulation from beam-beam interaction and unequal radio frequencies in RHIC", BNL CAD/AP/72 (2001).